

# Identification of a Novel Long Non-coding RNA, *lnc-ATMIN-4:2*, and its Clinicopathological and Prognostic Significance in Advanced Gastric Cancer

EOJIN KIM<sup>1</sup>, HYUNJIN KIM<sup>2</sup>, MIN-KYUNG YEO<sup>3</sup>, CHUL HWAN KIM<sup>4</sup>,  
JOO YOUNG KIM<sup>5</sup>, SUNGSOO PARK<sup>6</sup>, HYUN-SOO KIM<sup>7</sup> and YANG-SEOK CHAE<sup>1,4</sup>

<sup>1</sup>Department of Pathology, Korea University College of Medicine, Seoul, Republic of Korea;

<sup>2</sup>Pathology Center, Seegene Medical Foundation, Seoul, Republic of Korea;

<sup>3</sup>Department of Pathology, Chungnam National University School of Medicine, Daejeon, Republic of Korea;

<sup>4</sup>Department of Pathology, Anam Hospital, Korea University College of Medicine, Seoul, Republic of Korea;

<sup>5</sup>Department of Pathology, Kangnam Sacred Heart Hospital,

Hallym University College of Medicine, Seoul, Republic of Korea;

<sup>6</sup>Division of Foregut Surgery, Korea University College of Medicine, Seoul, Republic of Korea;

<sup>7</sup>Department of Pathology and Translational Genomics, Samsung Medical Center,

Sungkyunkwan University School of Medicine, Seoul, Republic of Korea

**Abstract.** *Background/Aim:* Long non-coding RNAs (lncRNAs) are emerging as significant regulators of gene expression and a novel promising biomarker for cancer diagnosis and prognosis. This study identified a novel, differentially expressed lncRNA in advanced gastric cancer (AGC), *lnc-ATMIN-4:2*, and evaluated its clinicopathological and prognostic significance. *Patients and Methods:* Whole transcriptome sequencing was performed to identify differentially expressed lncRNAs in AGC tissue samples. We also analyzed *lnc-ATMIN-4:2* expression in 317 patients with AGC using RNA *in situ* hybridization. *Results:* High (>30 dots) *lnc-ATMIN-4:2* expression significantly correlated with

younger age, poorly differentiated histology, diffuse type, deeper invasion depth, perineural invasion, lymph node metastasis, and higher stage group. In addition, high *lnc-ATMIN-4:2* expression was significantly associated with worse overall survival in patients with AGC. *Conclusion:* This study elucidated the significance of lncRNAs in AGC and indicated the value of *lnc-ATMIN-4:2* expression as a predictive biomarker for the overall survival of patients with AGC.

*Correspondence to:* Yang-Seok Chae, Department of Pathology, Anam Hospital, Korea University College of Medicine, 73, Incheon-ro, Seongbuk-gu, Seoul 02841, Republic of Korea. Tel: +82 29205595, Fax: +82 29205590, e-mail: chaes21@korea.ac.kr; Hyun-Soo Kim, Department of Pathology and Translational Genomics, Samsung Medical Center, Sungkyunkwan University School of Medicine, 81, Irwon-ro, Gangnam-gu, Seoul 06351, Republic of Korea. Tel: +82 234101243, Fax: +82 234142831, e-mail: hyun-soo.kim@samsung.com

**Key Words:** Stomach cancer, advanced gastric cancer, long non-coding RNA, *lnc-ATMIN-4:2*, whole transcriptome sequencing, RNA *in situ* hybridization, prognosis.

Gastric cancer is the fifth most common malignancy and the fourth leading cause of cancer death worldwide (1). According to global cancer statistics, gastric cancer accounted for over one million new cases (5.6% of all cancer diagnosed) and approximately 769,000 deaths in 2020 (2, 3). Even though advanced treatment approaches such as molecular-targeted therapies and immunotherapy exist, the standard treatment for gastric cancer is perioperative chemotherapy or surgery followed by postoperative chemotherapy (4). The prognosis of patients with gastric cancer remains unfavorable, with five-year overall survival (OS) rates of approximately 30% in Western countries (5). More than 70% of patients with gastric cancer fail to develop specific symptoms during the early stages, and the disease is diagnosed only in the advanced stages (4), denying the patients an opportunity to undergo the most effective surgical treatment (6). Owing to metastases to distant organs, the five-year OS rate of patients with gastric cancer diagnosed in advanced stages is <5% (7). Therefore, identifying potential biomarkers and drug targets is essential for providing novel diagnostic and therapeutic strategies and



This article is an open access article distributed under the terms and conditions of the Creative Commons Attribution (CC BY-NC-ND) 4.0 international license (<https://creativecommons.org/licenses/by-nc-nd/4.0>).

improving the clinical course and survival rate of patients with advanced gastric cancer (AGC).

With the advent of high-throughput sequencing technologies, most of the human genome was found to be actively transcribed into non-coding RNAs (8). Even though non-coding RNAs, including microRNAs and long non-coding RNAs (lncRNAs), do not encode any proteins, they play significant regulatory functions in the expression of other protein-coding genes (9). lncRNAs are a recently discovered class of non-coding RNAs ranging in length from 200 nucleotides to 100 kilobases (10) and play an essential role in the epigenetic, transcriptional, and post-transcriptional regulation of genes (11, 12). Functional *in vitro* studies and animal models have indicated that lncRNAs regulate various biological processes, including differentiation and development (13, 14). Interestingly, dysregulated lncRNAs were identified in various tumor tissues compared to corresponding normal tissues, implicating their crucial role in tumorigenesis, progression, and metastasis (15-19). Depending on the fold difference, genes differentially expressed in the normal and tumor tissues are considered candidate genes for biomarkers (20). Moreover, lncRNAs demonstrate cell-, tissue-, and disease-specific expression profiles than any protein-coding genes, suggesting the possible role of lncRNAs as promising biomarkers for cancer diagnosis and prognosis. Increasing evidence also reports a direct correlation between the expression of lncRNAs and the tumor status much better than that of protein-coding genes (21-26).

However, few studies have clinically validated lncRNA signature in AGC. This study compared the lncRNA expression profiles of AGC and normal gastric tissues. We conducted bioinformatic analyses to identify a novel lncRNA among the differentially expressed lncRNAs (DELncRNAs). In addition, we examined the expression of *lnc-ATMIN-4:2*, a novel lncRNA, in a large number of AGC tissue samples using tissue microarray (TMA) and RNA *in situ* hybridization (ISH) techniques. Finally, we assessed the clinicopathological and prognostic significance of the expression status of *lnc-ATMIN-4:2* in patients with AGC. This study identified and clinically validated the novel lncRNA, *lnc-ATMIN-4:2*, which could be a candidate prognostic biomarker for patients with AGC.

## Materials and Methods

**Case selection for whole-transcriptome sequencing.** The study protocol was approved by The Korea University Hospital Institutional Review Board (approval number: 2019AN0381). Six tissue samples, including three AGC and the corresponding three non-tumorous gastric tissues, were obtained from the Korea University Anam Hospital Biobank. The non-tumorous tissues were sampled at a significant distance from the tumor (>2 cm). The mean age of the patients with AGC was 65.3 years, with no history of preoperative treatment. Table I summarizes their clinicopathological

Table I. Clinicopathological information of three patients with advanced gastric cancer whose tissue samples were used for whole transcriptome sequencing.

Parameter	Sample ID		
	NvT 1	NvT 2	NvT 3
Age (years)	75	44	77
Sex	Male	Male	Male
Histological differentiation	Moderate	Poor	Poor
Lauren classification	Intestinal	Diffuse	Mixed
Tumor size (cm)	5.1	12.7	11.5
Pathological tumor stage (pT)	pT3	pT4a	pT4a
Lymphovascular invasion	Absent	Present	Present
Perineural invasion	Absent	Present	Absent
Lymph node metastasis	Present	Present	Present
Distant metastasis	Absent	Present	Present
Survival status	Alive	Dead	Alive

characteristics. One patient (normal *versus* tumor 1; NvT 1) was a 75-year-old man whose tumor was a 5.1-cm AGC involving the subserosa. He did not develop distant metastasis or local recurrence. The other two patients (NvT 2 and 3) had bulky tumors measuring >10 cm, pathological tumor stage (pT) of pT4, and demonstrated lymphovascular space invasion and distant metastasis.

**RNA isolation, library preparation, and whole transcriptome sequencing.** Total RNA was isolated using TRIzol Reagent (Invitrogen, Waltham, MA, USA). RNA quality was assessed by Agilent 2100 Bioanalyzer System (Agilent Technologies, Santa Clara, CA, USA) and RNA 6000 Nano Kit (Agilent Technologies). RNA quantification was performed using NanoDrop 2000 Spectrophotometer (Thermo Fisher Scientific, Waltham, MA, USA). Libraries were prepared from the total RNA using NEBNext Ultra II Directional RNA Library Prep Kit (New England Biolabs, Ipswich, MA, USA). Ribosomal RNA (rRNA) was removed using RiboCop rRNA Depletion Kit (Lexogen, Vienna, Austria). The rRNA-depleted RNAs were used for cDNA synthesis and shearing. Indexing was performed using Index Primer Set 1-12 (Illumina, San Diego, CA, USA). The enrichment step was conducted using polymerase chain reaction (PCR). Subsequently, libraries were analyzed using High Sensitivity DNA Kit (Agilent Technologies) to evaluate the mean fragment size. Quantification was performed using Colibri Library Quantification Kit (Invitrogen) and StepOne Real-Time PCR System (Thermo Fisher Scientific). High-throughput sequencing was conducted as paired-end 100 sequencing bp using NovaSeq 6000 Sequencing System (Illumina).

**Sequencing data processing.** Quality control of raw sequencing data was performed using FastQC (Babraham Institute, Cambridge, UK). Adapter and low-quality reads (<Q20) were removed using FASTX-Toolkit (Hannon Laboratory, Cold Spring Harbor Laboratory, Huntington, NY, USA) and BBMap (Joint Genome Institute, Berkeley, CA, USA). The trimmed reads were mapped to the reference genome using TopHat (Center for Bioinformatics and Computational Biology, College Park, MD, USA) (27). The expression levels of genes, isoforms, and lncRNAs were estimated using Cufflinks based fragments per kb of transcript per million

mapped fragment (FPKM) values (28). The FPKM values were normalized based on the quantile normalization method using edgeR. Data mining was performed using ExDEGA (Ebiogen, Seoul, Republic of Korea). The lncRNAs were selected for further analysis if their log2 fold changes were  $\geq 2.0$  or  $< 0.5$  and if normalized data were  $\geq 2.0$ .

**Gene Expression Omnibus (GEO) dataset collection for novel lncRNA validation.** Microarray datasets from the GEO database (National Institutes of Health, Bethesda, MD, USA) were collected and used to assess the differential expression of *lnc-ATMIN-4:2* (also known as NONHSAT143937.2, NONHSAG020094.2, ENST00000501068, and ENSG00000245059). The normalized probe-level intensity files (GSE50710, GSE53137, GSE109476, GSE95667, and GSE93512) were generated by Human Version 2.0 LncRNA Array (Arraystar, Rockville, MD, USA). A total of 27 gastric cancer samples and non-tumorous tissues were collected.

**Case selection for TMA construction and RNA ISH.** The study protocol was approved by The Korea University Hospital Institutional Review Board (approval number: 2020AN0544). We retrospectively retrieved all surgically resected cases of AGC between January 2009 and December 2012. Patients who received neoadjuvant chemotherapy were excluded from the study. A total of 317 cases of histologically confirmed AGC were included in this study. The following clinicopathological information was collected: age, sex, histological differentiation, Lauren classification, tumor size, pT, lymphovascular invasion, perineural invasion, lymph node metastasis, distant metastasis, local recurrence, and stage group. The latter was determined according to the eighth edition of the American Joint Committee on Cancer Staging Manual (29).

**TMA construction.** We constructed TMA blocks using AGC tissues as previously described (30). All available hematoxylin and eosin-stained slides were reviewed by two board-certified pathologists, and in each case, the most representative slide areas were marked on the corresponding formalin-fixed paraffin-embedded tissue (FFPE) block. For each case, two 3 mm-diameter cores were extracted from the FFPE block and manually arrayed into recipient TMA blocks. The percentage tumor volume in each core was  $>70\%$ .

**RNA ISH.** Single-color RNA ISH was performed using RNAscope 2.5 HD Reagent Kit-RED (Advanced Cell Diagnostics, Newark, CA, USA). Briefly, 4  $\mu\text{m}$ -thick TMA sections were deparaffinized in xylene, followed by dehydration in ethanol. Samples were incubated in citrate buffer, rinsed in water, and treated with Protease Plus (Advanced Cell Diagnostics) at  $40^\circ\text{C}$  for 30 min in a HybEZ Hybridization Oven (Advanced Cell Diagnostics). Samples were then incubated with a custom-designed sample probe, followed by Amplifier 1 (30 min), Amplifier 2 (15 min), Amplifier 3 (30 min), and Amplifier 4 (15 min) at  $40^\circ\text{C}$ . Amplifiers 5 (30 min) and 6 (15 min) were applied at room temperature. Chromogenic detection was performed using Fast Red dye, followed by counterstaining with hematoxylin. The stained sections were mounted with VectaMount Mounting Medium (Vector Laboratories, Burlingame, CA, USA). The control slide consisted of Human Hela Cell Pellet, and the probes used included a customized 7 ZZ probe named Hs-NONHSAT1439372 (Advanced Cell Diagnostics). Positive and negative control probes were hs-PPIB and dapB (Advanced Cell Diagnostics), respectively.

**RNA ISH interpretation.** The stained slides were scanned using PANNORAMIC 1000 digital slide scanner (3DHISTECH, Budapest, Hungary). Virtual slide files were opened using CaseViewer (3DHISTECH). Two microscopic areas showing the highest expression were captured at high-power magnification ( $400\times$ ) for each case, and the number of tumor cells and red dots were counted using CellProfiler Version 4.1.3 (Broad Institute, Cambridge, MA, USA). We calculated the number of red dots per 500 tumor cells in two high-power fields. A mean number of red dots was determined as the cut-off value for the dichotomizing *lnc-ATMIN-4:2* expression. The case showing  $>30$  dots was classified as a high *lnc-ATMIN-4:2* expression group. A 'very' high *lnc-ATMIN-4:2* expression was defined as  $>100$  dots.

**Statistical analysis.** The chi-square and Fisher's exact test were used to examine the association between *lnc-ATMIN-4:2* expression and clinicopathological parameters. The Kaplan–Meier plot and log-rank test were used to assess the difference in OS according to the *lnc-ATMIN-4:2* expression status. The Cox proportional hazards regression analysis was also used to evaluate the prognostic significance of *lnc-ATMIN-4:2* expression. A  $p$ -value  $< 0.05$  was considered statistically significant. These statistical analyses were performed using IBM SPSS Statistics for Windows, Version 27.0 (IBM, Armonk, NY, USA). Additionally, we used R software Version 4.1.1 (R Foundation for Statistical Computing, Vienna, Austria) and the DESeq Version 1.48.0 (R Foundation for Statistical Computing), an R package to identify differentially expressed genes or isoforms from different samples, to reveal DElncRNAs in the GEO database and our sequencing data (31–33). When identifying overlapped DElncRNAs in our data, a  $p$ -value  $< 0.001$  was considered statistically significant.

## Results

**Identification of DElncRNAs.** To identify DElncRNAs, we analyzed the whole transcriptomes of three AGCs and the matched normal gastric tissue samples (NvT 1, NvT 2, and NvT 3) and identified approximately 47,000 lncRNAs in each sample. A Venn diagram was constructed to illustrate the common and exclusive lncRNAs in three samples (Figure 1A), and our results identified fourteen up-regulated and three down-regulated lncRNAs in common. Heatmaps and hierarchical clustering revealed the expression profiles of these 17 commonly dysregulated lncRNAs (Figure 1B). Table II, Table III, and Table IV summarize the differential expression of lncRNAs in AGCs compared to normal controls in NvT 1, NvT 2, and NvT 3, respectively. In particular, three DElncRNAs, including NONHSAT143937.2, NONHSAT158405.1, and NONHSAT222425.1, were overlapped in all samples and were considered candidates for validation (Table V). The latter, a contra-regulated lncRNA, was excluded from further analysis. Two pT4 AGCs with unfavorable clinicopathological features, including larger tumor size, higher invasion depth, lymphovascular invasion, and distant metastasis, showed higher fold changes (15.769 and 15.619 in NvT 2 and NvT 3, respectively) of NONHSAT143937.2 than pT3 AGC tumor (NvT 1, 4.638). In contrast, the fold changes of

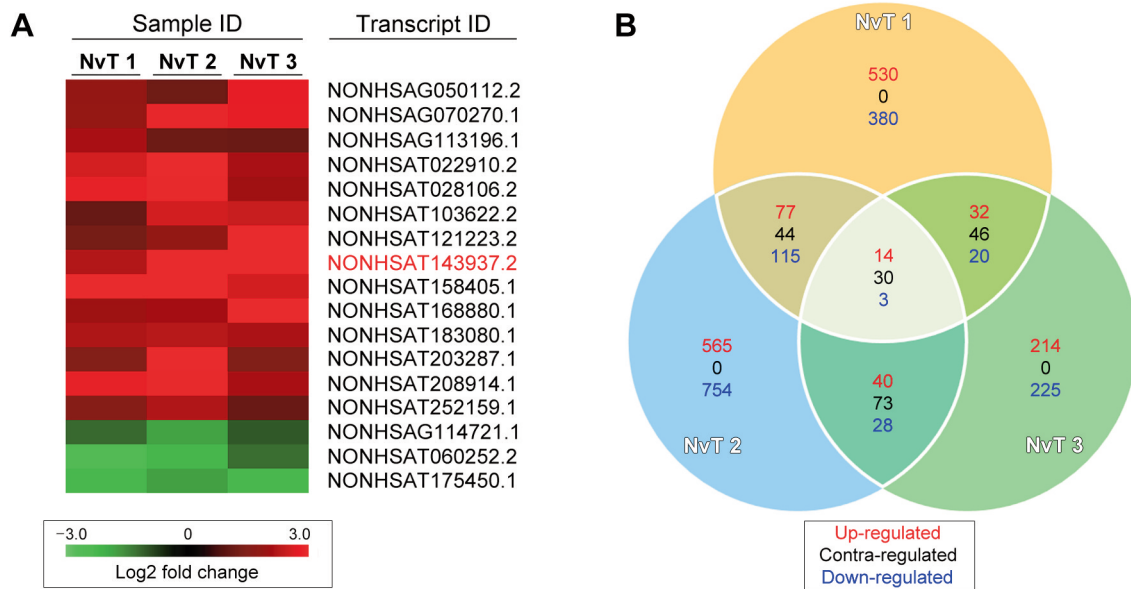


Figure 1. Overview of long non-coding RNAs (lncRNAs) identified in advanced gastric cancer (AGC). (A) Venn diagram illustrating the number of dysregulated lncRNAs in three AGC tissue samples (NvT 1-3). A total of 47 lncRNAs were found to overlap in all samples. Among these, 14 lncRNAs were up-regulated (red), and three were down-regulated (green). (B) Heatmap representing the expression profiles of the 17 overlapped lncRNAs across the samples. We found a novel lncRNA NONHSAT143937.2 (red), also known as lnc-ATMIN-4:2.

Table II. A list of differentially expressed long non-coding RNAs in patient NvT 1.

Transcript/gene ID	Tumor	Normal	Log2 (fold change)	Z-Score	p-Value	q-Value (32)	q-Value (33)	Signature ( $p < 0.001$ )
<b>NONHSAT158405.1</b>	50.23	3.91	3.683308762	7.382833414	<0.0000001	<0.0000001	<0.0000001	True
<b>NONHSAT143937.2</b>	68.21	13.81	2.304269943	7.269596939	<0.0000001	<0.0000001	<0.0000001	True
<b>NONHSAT222425.1</b>	0	15.79	-4.980939266	-3.902408099	0.0000952	0.001269872	0.001269872	True
NONHSAG011875.2	0	11.64	-4.541019153	-3.277446242	0.001047507	0.010475068	0.010475068	False
NONHSAG009745.2	0	10.84	-5.224168046	-3.255121431	0.001133439	0.009067511	0.009067511	False
NONHSAG059836.1	0	11.33	-4.502075956	-3.225666301	0.001256798	0.008378653	0.008378653	False
NONHSAT227214.1	38.87	80.98	-1.058908535	-3.189913175	0.001423155	0.008132317	0.008132317	False
NONHSAT122481.2	9.24	30.67	-1.73086341	-3.035510819	0.002401286	0.01200643	0.01200643	False
NONHSAG050112.2	13.10	2.88	2.185426095	2.998216637	0.002715646	0.012069536	0.012069536	False
NONHSAT174054.1	0	10.02	-4.324810603	-2.996874595	0.002727629	0.010910516	0.010910516	False
NONHSAT174964.1	1.67	13.26	-2.989160768	-2.927752188	0.00341422	0.012415347	0.012415347	False
NONHSAT106537.2	34.51	71.16	-1.044052037	-2.913204668	0.0035774	0.011924668	0.011924668	False
NONHSAG091124.1	7.46	0	3.89917563	2.844482508	0.004448363	0.01368727	0.01368727	False
NONHSAT021258.2	0	8.57	-4.099295204	-2.721600519	0.006496662	0.018561893	0.018561893	False
NONHSAG070270.1	9.92	1.97	2.332144491	2.690130869	0.0071424	0.019046401	0.019046401	False
NONHSAT028106.2	6.25	0	3.64385619	2.553688411	0.010658859	0.026647148	0.026647148	False
NONHSAT208914.1	6.23	0	3.639232163	2.548609594	0.01081533	0.025447835	0.025447835	False
NONHSAG034877.2	0	7.71	-3.94673086	-2.544961019	0.010928994	0.024286653	0.024286653	False
NONHSAG076398.1	0	6.97	-3.801158656	-2.383330037	0.017156805	0.036119589	0.036119589	False
NONHSAT158689.1	3.55	14.14	-1.99389119	-2.290547802	0.021989581	0.043979162	0.043979162	False
NONHSAG093134.1	0	6.35	-3.666756592	-2.239887983	0.025098196	0.047806088	0.047806088	False
NONHSAT252159.1	8.04	2	2.007195501	2.239472393	0.025125196	0.045682174	0.045682174	False
NONHSAG078089.1	5.02	0	3.327687364	2.221110091	0.026343506	0.045814793	0.045814793	False
NONHSAG059837.1	0	5.37	-3.424922088	-1.995198301	0.046021256	0.076702094	0.076702094	False
NONHSAT121223.2	7.99	2.65	1.592203143	1.960992659	0.049879879	0.079807807	0.079807807	False

Bold IDs indicate overlapped differential expressed long non-coding RNAs ( $p < 0.001$ ).



Table III. A list of differentially expressed long non-coding RNAs in patient NvT 2.

Transcript/gene ID	Tumor	Normal	Log2 (fold change)	Z-Score	p-Value	q-Value (32)	q-Value (33)	Signature ( $p < 0.001$ )
NONHSAT227214.1	9.59	101.21	-3.3996772	-9.2748817	<0.0000001	<0.0000001	<0.0000001	True
NONHSAT040488.2	49.1	0	6.61765112	7.49189894	<0.0000001	<0.0000001	<0.0000001	True
<b>NONHSAT222425.1</b>	21.98	0	5.45811948	5.07034304	0.0000004	0.0000050	0.0000050	True
NONHSAT174964.1	3.65	29.49	-3.0142575	-4.544265	0.0000055	0.0000524	0.0000524	True
<b>NONHSAT158405.1</b>	16.46	0	5.04089243	4.36493464	0.0000127	0.0000966	0.0000966	True
<b>NONHSAT143937.2</b>	14.42	0	4.84999926	4.06750474	0.0000475	0.0003010	0.0003010	True
NONHSAT175450.1	7.94	32.28	-2.0234297	-3.7013711	0.00021444	0.00116409	0.00116409	True
NONHSAG114721.1	6.72	28.36	-2.0773244	-3.5248306	0.00042375	0.00201283	0.00201283	True
NONHSAG076398.1	0	11.94	-4.5777309	-3.3805629	0.00072338	0.00305425	0.00305425	True
NONHSAT188018.1	0	11.59	-4.5348087	-3.3225135	0.0008921	0.00338999	0.00338999	True
NONHSAT121223.2	17.12	4.61	1.89284405	3.08636838	0.00202618	0.00699952	0.00699952	False
NONHSAG009745.2	8.31	0	4.74450836	3.07349906	0.00211564	0.00669954	0.00669954	False
NONHSAT239368.1	0	9.49	-4.2464081	-2.9497951	0.00317985	0.00929494	0.00929494	False
NONHSAG034877.2	0	9.47	-4.2433644	-2.9460181	0.00321894	0.00873711	0.00873711	False
NONHSAG059836.1	7.94	0	3.98913901	2.90175884	0.00371074	0.00940054	0.00940054	False
NONHSAT208914.1	6.88	0	6.42626475	2.79825543	0.00513795	0.01220262	0.01220262	False
NONHSAT022910.2	7.24	0	3.8559897	2.74477105	0.00605531	0.0135354	0.0135354	False
NONHSAT203287.1	7.01	0	3.80941444	2.69121096	0.00711932	0.01502967	0.01502967	False
NONHSAT028106.2	6.64	0	3.73118324	2.6027939	0.00924675	0.0184935	0.0184935	False
NONHSAG011875.2	0	7.68	-3.9411063	-2.5864467	0.00969712	0.01842452	0.01842452	False
NONHSAT122481.2	6.55	0	3.71149491	2.58084387	0.00985591	0.01783451	0.01783451	False
NONHSAG070270.1	6.46	0	3.69153416	2.55871286	0.01050605	0.01814681	0.01814681	False
NONHSAT107049.2	2.8	13.06	-2.2216562	-2.4788588	0.01318035	0.02177622	0.02177622	False
NONHSAG059837.1	5.91	19.05	-1.688561	-2.4415112	0.01462594	0.02315773	0.02315773	False
NONHSAG048940.2	5.77	0	3.52857132	2.38257806	0.01719189	0.02613167	0.02613167	False
NONHSAG078089.1	5.16	0	3.36737107	2.21609904	0.02668472	0.03826488	0.03826488	False
NONHSAT174054.1	5.16	0	3.36737107	2.21609904	0.02668472	0.03826488	0.03826488	False
NONHSAT176868.1	0	6.06	-3.5993178	-2.214969	0.02676219	0.03632011	0.03632011	False
NONHSAT197026.1	11.16	4.03	1.46948528	2.12812486	0.03332673	0.04366951	0.04366951	False
NONHSAT228137.1	0	4.31	-5.7515441	-2.094022	0.03625802	0.04592683	0.04592683	False

Bold IDs indicate overlapped differential expressed long non-coding RNAs ( $p < 0.001$ ).

NONHSAT158405.1 in NvT 3 (5.903) were lower than that in NvT 1 (10.346). The differences in fold changes of NONHSAT143937.2 better reflected the oncogenic behavior in NvT 1, NvT 2, and NvT 3 than NONHSAT158405.1.

**Bioinformatic analysis for *lnc-ATMIN-4:2* validation.** We identified NONHSAT143937.2 as *lnc-ATMIN-4:2* (LNCipedia transcript ID), *lnc-ATMIN-4* (LNCipedia gene ID), ENSG00000245059 (Ensembl gene ID), and ENST00000501068 (Ensembl transcript ID), and validated the novel lncRNA using GEO database (National Institutes of Health). The results showed five datasets, including GSE50710, GSE53137, GSE109476, GSE95667, and GSE93512, containing 27 pairs of gastric cancer and normal gastric tissues. As shown in Table VI, in 10 of the 27 cases (37.0%), gastric cancer tissues showed higher *lnc-ATMIN-4:2* expression than normal tissues.

**Patient demographics.** This study included 205 males (64.7%) and 112 females (35.3%). The mean age of patients

was 60.3 years (range=26-87). Twenty-nine (9.1%), 107 (33.8%), and 181 (57.1%) patients were diagnosed with well, moderately, and poorly differentiated adenocarcinoma, respectively. According to the Lauren classification, 166 (52.4%) cases were diffuse type. Tumors measuring >6 cm were in 124 (39.1%) cases. Seventy-one (22.4%) cases were pT2 tumors, 155 (48.9%) were pT3, and 91 (28.7%) were pT4. Eighty-eight (27.8%) and 188 (59.3%) cases showed perineural and lymphovascular invasion, respectively. Two hundred and 29 patients (72.2%) had lymph node metastases. Nineteen patients (6.0%) developed distant metastases. The median follow-up time was 43 months (range=1-99).

**Clinicopathological and prognostic significance of *lnc-ATMIN-4:2*.** RNA ISH was performed to examine the *lnc-ATMIN-4:2* expression and to evaluate its clinicopathological and prognostic significance in 317 patients with AGC. The mean number of *lnc-ATMIN-4:2*-positive red dots per 500 tumor cells ranged 0.4-295.1 (mean=32.2 dots). Low *lnc-ATMIN-4:2*

Table IV. A list of differentially expressed long non-coding RNAs in patient NvT 3.

Transcript/gene ID	Tumor	Normal	Log2 (fold change)	Z-Score	p-Value	q-Value (32)	q-Value (33)	Signature ( $p < 0.001$ )
NONHSAT040488.2	0	107.392	-7.74674	-10.3825	<0.0000001	<0.0000001	<0.0000001	True
NONHSAT122481.2	14.53	0	4.861161	3.97061	0.0000717	0.0012904	0.0012904	True
<b>NONHSAT143937.2</b>	13.93	0	4.799813	3.87902	0.0001049	0.0012585	0.00125854	True
NONHSAT121223.2	12.71	0	4.667324	3.686361	0.0002275	0.0020473	0.00204735	True
NONHSAT158689.1	0	11.22	-4.48787	-3.36879	0.000755	0.0054359	0.00543593	True
<b>NONHSAT158405.1</b>	13.58	1.59	3.097594	3.350773	0.0008059	0.0048352	0.00483518	True
<b>NONHSAT222425.1</b>	0	10.94	-4.45088	-3.31918	0.0009028	0.004643	0.00464302	True
NONHSAT098836.2	0	10.58	-4.40313	-3.25589	0.0011304	0.0050866	0.00508663	False
NONHSAG078089.1	0	10.30	-4.36373	-3.20429	0.0013539	0.0054158	0.00541577	False
NONHSAG009745.2	8.31	0	4.821134	2.991728	0.002774	0.0099865	0.00998653	False
NONHSAT168880.1	8.60	0	4.104169	2.941169	0.0032698	0.010701	0.01070104	False
NONHSAG076398.1	6.52	0	3.705536	2.479692	0.0131496	0.0394488	0.03944875	False
NONHSAT227214.1	14.86	4.80	1.63154	2.430665	0.0150711	0.0417354	0.04173542	False
NONHSAT021258.2	8.53	1.64	2.376382	2.314457	0.0206427	0.0530812	0.05308115	False
NONHSAG070270.1	5.79	0	3.533563	2.295996	0.0216761	0.0520226	0.05202262	False
NONHSAG050112.2	5.73	0	3.51929	2.281147	0.0225397	0.0507144	0.05071438	False
NONHSAT203178.1	0	6.47	-9.48851	-2.27467	0.0229259	0.0485491	0.04854906	False
NONHSAT208914.1	5.01	0	3.524571	2.131826	0.0330212	0.0660424	0.06604237	False
NONHSAG000979.2	1.20	6.49	-2.43527	-1.96853	0.049007	0.0928554	0.09285536	False

Bold IDs indicate overlapped differentially expressed long non-coding RNAs ( $p < 0.001$ ).

Table V. Three overlapped differentially expressed long non-coding RNAs.

Transcript ID	NONHSAT143937.2	NONHSAT158405.1	NONHSAT222425.1
NONCODE gene ID	NONHSAG020094.2	NONHSAG062307.2	NONHSAG103252.1
Ensembl transcript ID	ENST00000501068	Not applicable	Not applicable
Ensembl gene ID	ENSG00000245059	Not applicable	Not applicable
Location (GRCh38)	chr16:81077319-81078861	chr10:91162363-91162680	chrM:10913-12049
LNCipedia transcript ID	<i>lnc-ATMIN-4:2</i>	Not applicable	Not applicable
LNCipedia gene ID	<i>lnc-ATMIN-4</i>	Not applicable	Not applicable
Length	1088	317	400
Class	lincRNA	lincRNA	lincRNA
Fold change			
NvT 1	4.638	10.346	0.059
NvT 2	15.769	17.836	23.419
NvT 3	15.619	5.903	0.087
Expression trend	Up-regulated	Up-regulated	Contra-regulated

GRCh38: Genome Reference Consortium Human Build 38; lincRNA: long intergenic non-coding RNA.

expression ( $\leq 30$  dots) was identified in 221 cases of AGC (69.7%; Figure 2A), while 96 cases (30.3%) exhibited high *lnc-ATMIN-4:2* expression ( $> 30$  dots; Figure 2B). Among these, very high expression of *lnc-ATMIN-4:2* expression ( $> 100$  dots) was observed in 25 cases (7.8%). High *lnc-ATMIN-4:2* expression was significantly associated with younger age ( $p = 0.007$ ) and unfavorable clinicopathological parameters, including poorly differentiated histology ( $p = 0.047$ ), diffuse type ( $p = 0.012$ ), deeper invasion depth ( $p = 0.002$ ), presence of perineural invasion ( $p = 0.017$ ), lymph node metastasis ( $p = 0.012$ ), and higher stage group ( $p = 0.004$ ) (Table VII).

OS of patients with AGC whose tumors showed high *lnc-ATMIN-4:2* expression was significantly lower than that of *lnc-ATMIN-4:2*-low AGC patients ( $p = 0.034$ ; Figure 2C). When the cases were classified into very high, high, and low expression subgroups, the difference in OS was also significant ( $p = 0.024$ ; Figure 2D). Cox regression analysis revealed that AGCs showing high *lnc-ATMIN-4:2* expression had significantly worse OS than those with low expression [hazard ratio (HR)=1.678; 95% confidence interval (CI)=1.034-2.724;  $p = 0.036$ ]. Other clinicopathological parameters associated with worse OS were diffuse type (HR=1.865; 95% CI=1.136-3.062;

Table VI. Differential expression of *lnc-ATMIN-4:2* in gastric cancer data obtained from the Gene Expression Omnibus database.

Sample ID	Tumor	Normal	Log2 (fold change)	Z-Score	p-Value	q-Value (32)	q-Value (33)	Signature ( $p < 0.05$ )
<b>GSE50710_1</b>	133.96	40.21	1.7361940	6.4197039	<0.0000001	<0.0000001	<0.0000001	True
<b>GSE95667_4</b>	164.57	80.38	1.0337931	4.3163722	0.0000159	0.0001071	0.0001071	True
<b>GSE50710_2</b>	88.30	35.15	1.3288874	4.0561953	0.0000499	0.0002245	0.0002245	True
<b>GSE109476_4</b>	83.98	33.62	1.3205630	3.9288486	0.0000854	0.0003292	0.0003292	True
<b>GSE53137_5</b>	167.37	95.55	0.8087576	3.2576346	0.0011234	0.0030333	0.0030333	True
<b>GSE93512_2</b>	10.96	0.82	3.7332011	2.9774149	0.0029069	0.0071351	0.0071351	True
<b>GSE53137_6</b>	162.76	99.16	0.7148767	2.7296715	0.0063397	0.0122267	0.0122267	True
<b>GSE95667_1</b>	138.64	82.40	0.7507060	2.6777118	0.0074127	0.0133429	0.0133429	True
<b>GSE50710_3</b>	51.067	25.82	0.9840086	2.2301229	0.0257393	0.0408800	0.0408800	True
<b>GSE109476_1</b>	79.93	46.23	0.7898248	2.1484781	0.0316758	0.0450130	0.0450130	True
GSE53137_1	67.42	127.14	-0.9152692	-5.5657089	0.0000000	0.0000004	0.0000004	False
GSE95667_2	45.42	97.86	-1.1074114	-5.4756353	0.0000000	0.0000004	0.0000004	False
GSE50710_8	30.93	63.53	-1.0382093	-4.2120491	0.0000253	0.0001367	0.0001367	False
GSE50710_6	38.57	68.06	-0.8192558	-3.7568759	0.0001720	0.0005807	0.0005807	False
GSE109476_3	96.72	132.76	-0.4569252	-3.7268853	0.0001939	0.0005816	0.0005816	False
GSE50710_7	46.38	67.39	-0.5390098	-2.8861073	0.0039004	0.0087759	0.0087759	False
GSE109476_5	48.31	69.28	-0.5201743	-2.8659876	0.0041571	0.0086340	0.0086340	False
GSE95667_3	66.37	84.79	-0.3533500	-2.5549897	0.0106191	0.0179197	0.0179197	False
GSE50710_4	70.36	84.25	-0.2598555	-2.1794046	0.0293016	0.0439524	0.0439524	False
GSE53137_2	158.56	108.34	0.5494531	1.8152027	0.0694928	0.0938152	0.0938152	False
GSE50710_10	84.37	92.25	-0.1287780	-1.7219009	0.0850875	0.1093982	0.1093982	False
GSE50710_9	78.95	86.86	-0.1378693	-1.7074617	0.0877363	0.1076763	0.1076763	False
GSE109476_2	38.56	40.31	-0.0647293	-0.9379389	0.3482758	0.4088455	0.4088455	False
GSE53137_3	112.10	106.57	0.0729477	-0.8633074	0.3879685	0.4364645	0.4364645	False
GSE50710_5	61.52	44.34	0.4724728	0.8470295	0.3969787	0.4287370	0.4287370	False
GSE53137_4	147.04	117.07	0.3288176	0.5348823	0.5927312	0.6155286	0.6155286	False
GSE93512_1	11.26	8.53	0.4005440	0.2523557	0.8007662	0.8007662	0.8007662	False

Bold IDs indicate cases showing significantly up-regulated *lnc-ATMIN-4:2* expression ( $p < 0.05$ ).

$p=0.014$ ), larger tumor size (HR=2.843; 95% CI=1.761-4.588;  $p<0.001$ ), higher pT (HR=3.702; 95% CI=2.279-6.013;  $p<0.001$ ), lymphovascular invasion (HR=2.675; 95% CI=1.544-4.634;  $p<0.001$ ), perineural invasion (HR=2.242; 95% CI=1.378-3.650;  $p=0.001$ ), lymph node metastasis (HR=2.301; 95% CI=1.255-4.219;  $p=0.007$ ), and higher stage group (HR=3.453; 95% CI=1.966-6.062;  $p<0.001$ ).

## Discussion

With the high-throughput sequencing technologies of the whole human mammalian transcriptomes, it became evident that only 20,000 genes (<2%) are protein-coding, while at least 75% are actively transcribed into non-coding RNAs (34-37). Identifying aberrant expression of specific lncRNAs could be exploited to develop novel diagnostic biomarkers and may be associated with aggressive oncogenic behavior and poor patient outcomes (38). Therefore, an in-depth understanding of the mechanisms of lncRNA dysregulation may provide a better therapeutic strategy. According to a recent meta-analysis on lncRNAs, in a total of 6,095 gastric cancer patients (39), the expression of 19 lncRNAs is documented in 51 articles.

Most of these candidate lncRNAs efficiently predicted the prognosis of patients with AGCs, and included actin filament-associated protein 1 antisense RNA 1 (*AFAP-AS1*), colon cancer-associated transcript 2 (*CCAT2*), homeobox A transcript antisense RNA (*HOTAIR*), homeobox A transcript cluster distal transcript antisense RNA (*HOTTIP*), long intergenic non-protein-coding RNA 673 (*LINC00673*), metastasis-associated lung adenocarcinoma transcript 1 (*MALAT1*), promoter of cyclin-dependent kinase inhibitor 1A antisense DNA damage activated RNA (*PANDAR*), plasmacytoma variant translocation 1, (*PVT1*) sex-determining region Y-box 2 overlapping transcript (*Sox2ot*), zinc finger E-box binding homeobox 1-antisense RNA 1 (*ZEB1-AS1*), zinc finger nuclear transcription factor, and X box binding, and 1-type containing 1 antisense RNA 1 (*ZFAS1*) (35, 39-41). However, the smaller sample size available for the validation and the lack of reliability in the prognostic prediction of AGC pose a concern and are considered limitations. To the best of our knowledge, we identified for the first time a novel lncRNA, *lnc-ATMIN-4:2*, in AGC. We performed RNA ISH to determine the expression of *lnc-ATMIN-4:2* in 317 AGC tissue samples and demonstrated its clinicopathological and



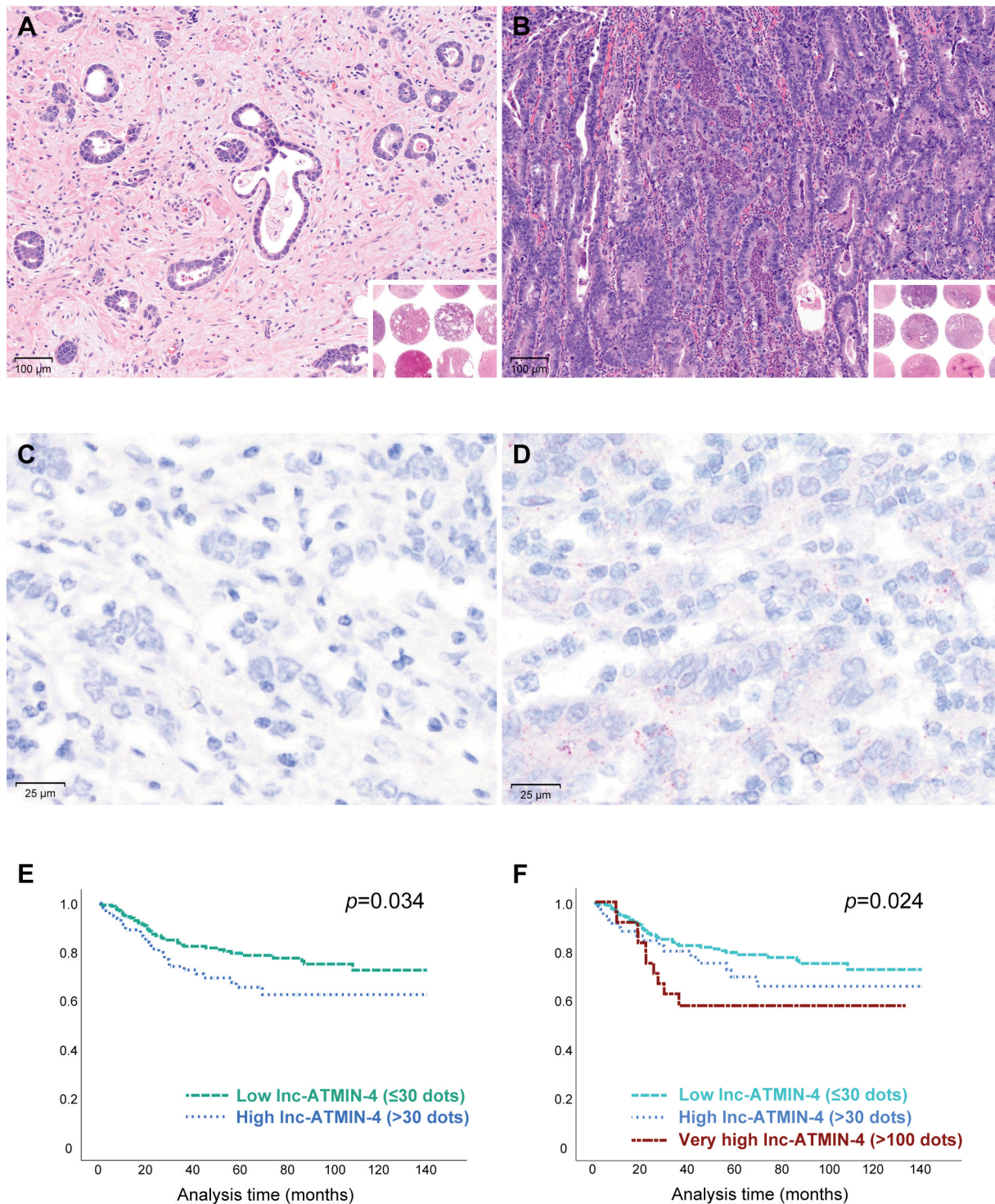


Figure 2. *Inc-ATMIN-4:2* expression evaluated by RNA in situ hybridization and its prognostic significance in patients with advanced gastric cancer (AGC). (A-B) Representative images of hematoxylin-and-eosin-stained AGC sections obtained from the tissue microarray blocks (inset in the right lower corner). Original magnification: 100 $\times$ . Representative RNA in situ hybridization images of (C) low *Inc-ATMIN-4:2* expression and (D) high *Inc-ATMIN-4:2* expression visualized as punctate red dots. Original magnification: 400 $\times$ . (E) Kaplan-Meier plots showing a significantly lower overall survival rate of patients with AGC whose tumors exhibit high *Inc-ATMIN-4:2* than that of *Inc-ATMIN-4:2*-low AGC patients ( $p=0.034$ ). (F) Kaplan-Meier plots showing significant differences ( $p=0.024$ ) in overall survival between patients with AGC exhibiting low, high, and very high *Inc-ATMIN-4:2* expression.



Table VII. Clinicopathological significance of *lnc-ATMIN-4:2* expression status in advanced gastric cancer.

Parameter	Number of cases (%)			<i>p</i> -Value
	Total	<i>lnc-ATMIN-4:2</i> expression status		
		Low	High	
Age (years)				
≤60	160	101 (31.9)	59 (18.6)	<b>0.007</b>
>60	157	120 (37.9)	37 (11.7)	
Sex				
Male	205	145 (45.7)	60 (18.9)	0.341
Female	112	76 (24.0)	36 (11.4)	
Histological differentiation				
Well	29	20 (6.3)	9 (2.8)	<b>0.047</b>
Moderate	107	84 (26.5)	23 (7.3)	
Poor	181	117 (36.9)	64 (20.2)	
Lauren classification				
Intestinal	151	115 (36.3)	36 (11.4)	<b>0.012</b>
Diffuse	166	106 (33.4)	60 (18.9)	
Tumor size (cm)				
≤6	193	137 (43.2)	56 (17.7)	0.312
>6	124	84 (26.5)	40 (12.6)	
Pathological tumor stage (pT)				
pT2	71	60 (18.9)	11 (3.5)	<b>0.002</b>
pT3	155	107 (33.8)	48 (15.1)	
pT4	91	54 (17.0)	37 (11.7)	
Lymphovascular invasion				
Absent	129	92 (29.0)	37 (11.7)	0.349
Present	188	129 (40.7)	59 (18.6)	
Perineural invasion				
Absent	229	168 (53.0)	61 (19.2)	<b>0.017</b>
Present	88	53 (16.7)	35 (11.0)	
Lymph node metastasis				
Absent	88	70 (22.1)	18 (5.7)	<b>0.012</b>
Present	229	151 (47.6)	78 (24.6)	
Distant metastasis				
Absent	298	211 (66.6)	87 (27.4)	0.082
Present	19	10 (3.2)	9 (2.8)	
Stage group				
I	44	39 (12.3)	5 (1.6)	<b>0.004</b>
II	88	65 (20.5)	23 (7.3)	
III	174	112 (35.3)	62 (19.6)	
IV	11	5 (1.6)	6 (1.9)	

Bold values indicate statistical significance ( $p < 0.05$ ).

prognostic significance. We observed that high *lnc-ATMIN-4:2* expression significantly correlated with younger age, diffuse type of Lauren classification, deeper invasion depth, perineural invasion, lymph node metastasis, and higher stage group. Survival analysis revealed that patients with AGC, whose tumors exhibit high and a “very” high *lnc-ATMIN-4:2* expression, had significantly worse OS than patients with *lnc-ATMIN-4:2*-low AGC.

The *lnc-ATMIN-4:2* is located on chromosome 16q23.2, and its biological function remains largely unknown. Nevertheless, DIANA-LncBase Version 3.0 (<https://diana.e-ce.uth.gr/lncbasev3>; University of Thessaly, Volos, Greece) suggested a potential miRNA-lncRNA interaction between *microRNA-34a* (*miR-34a*) and *lnc-ATMIN-4:2* in human colorectal carcinoma cell line HCT116 (42). The lncRNAs are known to interact with DNA and proteins, alter gene expression, and play a vital role in tumorigenesis (43, 44). Dysregulated *miR-34a* has been associated with epithelial–mesenchymal transition, tumor progression, and metastasis in many types of human cancers (45, 46). Moreover, *miR-34a* has been reported to have the potential to serve as diagnostic and prognostic biomarker in various human cancers, including gastric (47–50) and breast cancers (51, 52). In this study, however, we failed to observe any evidence of *miR-34a* dysregulation or its interaction with lncRNA in our sequencing data. Further investigation is essential to validate the mechanism of lncRNA:miR regulation in AGC associated with *lnc-ATMIN-4:2*.

To understand the lncRNA-protein molecular interactions, we sought for proteins potentially interacting with *lnc-ATMIN-4:2* using RNAc, a database of the RNA–protein interactome, and catRAPID, a computationally expensive method for predicting potential lncRNA-protein interactions (53). The following seven protein-coding genes were implicated in strong positive prediction and expressed aberrantly in human cancers: *nischarin* (*NISCH*), *retinoblastoma 1* (*RB1*)-inducible coiled-coil 1 (*RB1CC1*), ATP-binding cassette, sub-family C member 9 (*ABCC9*), damage-specific DNA binding protein 1 and cullin 4-associated factor 8 like 2 (*DCAF8L2*), DnaJ heat shock protein family member C5 beta (*DNAJC5B*), zinc finger CCHC-type containing 6 (*ZCCHC6*), and bromodomain-containing protein 4-interacting chromatin remodeling complex-associated protein (*BICRA*). *NISCH*, a tumor suppressor gene, was significantly down-regulated in advanced-stage ovarian cancer (49). *RB1CC1* is also a tumor suppressor gene that regulates *RB1* protein expression and activates the p16 promoter to enhance the *RB1* pathway (54). The immunohistochemical expression of nuclear *RB1CC1* protein significantly correlated with *RB1* expression in breast cancer tissue samples (55). *ABCC9* expression varied among different tissues and organs. High *ABCC9* expression was significantly associated with poor prognosis in gastric cancer patients (53), while this gene was significantly down-regulated in prostate (56), ovarian (57), and breast cancers (58). The *DCAF8L2*, *DNAJC5*, *ZCCHC6*, and *BICRA* genes were aberrantly over-expressed in various human cancers (59–62). Further experimental and molecular verifications for these cancer-related genes are required to disclose the potential RNA-protein interactions and their mechanisms.

Our study had a few limitations. First, we investigated DElncRNAs in three AGCs and matched normal gastric tissue samples. The small number of cases for whole-transcriptome sequencing may be a limit to reliable results. However, to

compensate for this limitation, we collected the data on *lnc-ATMIN-4:2* expression in gastric cancer from the GEO database. Analysis of the five GEO datasets revealed high *lnc-ATMIN-4:2* expression in 10 of the 27 gastric cancer cases (37.0%). Second, the GEO datasets did not consist exclusively of AGC cases. Even though the cases labeled as early gastric cancer were eliminated, we could not completely rule out the possible presence of early-stage disease due to the insufficient clinical information. To validate the up-regulated *lnc-ATMIN-4:2* expression in AGC, we performed RNA ISH using TMA blocks containing more than 300 cases of AGC. We observed 30.3% (96/317) of the cases displaying high *lnc-ATMIN-4:2* expression, which was a similar percentage to that observed in the result of GEO database analysis. Significant associations of high *lnc-ATMIN-4:2* expression with adverse clinicopathological parameters and worse survival of patients with AGC were noted.

In conclusion, we identified a novel lncRNA, *lnc-ATMIN-4:2*, in AGC tissues. Further, we demonstrated that high *lnc-ATMIN-4:2* expression determined by RNA ISH was associated with unfavorable clinicopathological parameters and could predict the OS of patients with AGC. Our observations suggest that *lnc-ATMIN-4:2* expression status could be used as a novel prognostic biomarker for patients with AGC. Further studies are warranted to clarify the biological function of *lnc-ATMIN-4:2* in gastric cancer.

### Data Availability

The dataset has been deposited to the National Center for Biotechnology Information (NCBI) Gene Expression Omnibus (GEO) located at: <https://www.ncbi.nlm.nih.gov/geo/query/acc.cgi?acc=GSE210909>

### Conflicts of Interest

The Authors have no conflicts of interest to declare.

### Authors' Contributions

All Authors made substantial contributions to the conceptualization and design of the study; the acquisition, analysis, interpretation, and validation of the data; drafting of the article; critical revision of the article for important intellectual content; and the final approval of the version to be published.

### Acknowledgements

This research was supported by the Bio and Medical Technology Development Program of the National Research Foundation (NRF) funded by the Korean government (MSIT) (2019M3E5D1A02068558) and a grant of the Korea Health Technology R&D Project through the Korea Health Industry Development Institute (KHIDI) funded by Ministry of Health & Welfare, Republic of Korea (HR20C0025).

### References

- Bray F, Ferlay J, Soerjomataram I, Siegel RL, Torre LA and Jemal A: Global cancer statistics 2018: GLOBOCAN estimates of incidence and mortality worldwide for 36 cancers in 185 countries. *CA Cancer J Clin* 68(6): 394-424, 2018. PMID: 30207593. DOI: 10.3322/caac.21492
- Sung H, Ferlay J, Siegel RL, Laversanne M, Soerjomataram I, Jemal A and Bray F: Global cancer statistics 2020: GLOBOCAN estimates of incidence and mortality worldwide for 36 cancers in 185 countries. *CA Cancer J Clin* 71(3): 209-249, 2021. PMID: 33538338. DOI: 10.3322/caac.21660
- Wong MCS, Huang J, Chan PSF, Choi P, Lao XQ, Chan SM, Teoh A and Liang P: Global incidence and mortality of gastric cancer, 1980-2018. *JAMA Netw Open* 4(7): e2118457, 2021. PMID: 34309666. DOI: 10.1001/jamanetworkopen.2021.18457
- Song Z, Wu Y, Yang J, Yang D and Fang X: Progress in the treatment of advanced gastric cancer. *Tumour Biol* 39(7): 1010428317714626, 2017. PMID: 28671042. DOI: 10.1177/1010428317714626
- Siegel RL, Miller KD, Fuchs HE and Jemal A: Cancer statistics, 2022. *CA Cancer J Clin* 72(1): 7-33, 2022. PMID: 35020204. DOI: 10.3322/caac.21708
- Van Cutsem E, Sagaert X, Topal B, Haustermans K and Prenen H: Gastric cancer. *Lancet* 388(10060): 2654-2664, 2016. PMID: 27156933. DOI: 10.1016/S0140-6736(16)30354-3
- Asplund J, Kauppila JH, Mattsson F and Lagergren J: Survival trends in gastric adenocarcinoma: a population-based study in Sweden. *Ann Surg Oncol* 25(9): 2693-2702, 2018. PMID: 29987609. DOI: 10.1245/s10434-018-6627-y
- Wright MW and Bruford EA: Naming 'junk': human non-protein coding RNA (ncRNA) gene nomenclature. *Hum Genomics* 5(2): 90-98, 2011. PMID: 21296742. DOI: 10.1186/1479-7364-5-2-90
- Yan X, Ma L and Yang M: Identification and characterization of long non-coding RNA (lncRNA) in the developing seeds of *Jatropha curcas*. *Sci Rep* 10(1): 10395, 2020. PMID: 32587349. DOI: 10.1038/s41598-020-67410-x
- Ulitsky I and Bartel DP: lincRNAs: genomics, evolution, and mechanisms. *Cell* 154(1): 26-46, 2013. PMID: 23827673. DOI: 10.1016/j.cell.2013.06.020
- Hung T and Chang HY: Long noncoding RNA in genome regulation: prospects and mechanisms. *RNA Biol* 7(5): 582-585, 2010. PMID: 20930520. DOI: 10.4161/rna.7.5.13216
- Khorkova O, Hsiao J and Wahlestedt C: Basic biology and therapeutic implications of lncRNA. *Adv Drug Deliv Rev* 87: 15-24, 2015. PMID: 26024979. DOI: 10.1016/j.addr.2015.05.012
- Rinn JL and Chang HY: Genome regulation by long noncoding RNAs. *Annu Rev Biochem* 81: 145-166, 2012. PMID: 22663078. DOI: 10.1146/annurev-biochem-051410-092902
- Batista PJ and Chang HY: Long noncoding RNAs: cellular address codes in development and disease. *Cell* 152(6): 1298-1307, 2013. PMID: 23498938. DOI: 10.1016/j.cell.2013.02.012
- Prensner JR and Chinnaiyan AM: The emergence of lncRNAs in cancer biology. *Cancer Discov* 1(5): 391-407, 2011. PMID: 22096659. DOI: 10.1158/2159-8290.CD-11-0209
- Zhang H, Chen Z, Wang X, Huang Z, He Z and Chen Y: Long non-coding RNA: a new player in cancer. *J Hematol Oncol* 6: 37, 2013. PMID: 23725405. DOI: 10.1186/1756-8722-6-37
- Li S, Li B, Zheng Y, Li M, Shi L and Pu X: Exploring functions of long noncoding RNAs across multiple cancers through co-

- expression network. *Sci Rep* 7(1): 754, 2017. PMID: 28389669. DOI: 10.1038/s41598-017-00856-8
- 18 Wang C, Qi S, Xie C, Li C, Wang P and Liu D: Upregulation of long non-coding RNA XIST has anticancer effects on epithelial ovarian cancer cells through inverse downregulation of hsa-miR-214-3p. *J Gynecol Oncol* 29(6): e99, 2018. PMID: 30207107. DOI: 10.3802/jgo.2018.29.e99
  - 19 Oh EJ, Kim SH, Yang WI, Ko YH and Yoon SO: Long non-coding RNA HOTAIR expression in diffuse large B-cell lymphoma: in relation to polycomb repressive complex pathway proteins and H3K27 trimethylation. *J Pathol Transl Med* 50(5): 369-376, 2016. PMID: 27550047. DOI: 10.4132/jptm.2016.06.06
  - 20 MAQC Consortium, Shi L, Reid LH, Jones WD, Shippy R, Warrington JA, Baker SC, Collins PJ, de Longueville F, Kawasaki ES, Lee KY, Luo Y, Sun YA, Willey JC, Setterquist RA, Fischer GM, Tong W, Dragan YP, Dix DJ, Frueh FW, Goodsaid FM, Herman D, Jensen RV, Johnson CD, Lobenhofer EK, Puri RK, Schrf U, Thierry-Mieg J, Wang C, Wilson M, Wolber PK, Zhang L, Amur S, Bao W, Barbacioru CC, Lucas AB, Bertholet V, Boysen C, Bromley B, Brown D, Brunner A, Canales R, Cao XM, Cebula TA, Chen JJ, Cheng J, Chu TM, Chudin E, Corson J, Corton JC, Croner LJ, Davies C, Davison TS, Delenstarr G, Deng X, Dorris D, Eklund AC, Fan XH, Fang H, Fulmer-Smentek S, Fuscoe JC, Gallagher K, Ge W, Guo L, Guo X, Hager J, Haje PK, Han J, Han T, Harbottle HC, Harris SC, Hatchwell E, Hauser CA, Hester S, Hong H, Hurban P, Jackson SA, Ji H, Knight CR, Kuo WP, LeClerc JE, Levy S, Li QZ, Liu C, Liu Y, Lombardi MJ, Ma Y, Magnuson SR, Maqsodi B, McDaniel T, Mei N, Myklebost O, Ning B, Novoradovskaya N, Orr MS, Osborn TW, Papallo A, Patterson TA, Perkins RG, Peters EH, Peterson R, Philips KL, Pine PS, Pusztai L, Qian F, Ren H, Rosen M, Rosenzweig BA, Samaha RR, Schena M, Schroth GP, Shchegrova S, Smith DD, Staedtler F, Su Z, Sun H, Szallasi Z, Tezak Z, Thierry-Mieg D, Thompson KL, Tikhonova I, Turpaz Y, Vallanat B, Van C, Walker SJ, Wang SJ, Wang Y, Wolfinger R, Wong A, Wu J, Xiao C, Xie Q, Xu J, Yang W, Zhang L, Zhong S, Zong Y and Slikker W Jr: The MicroArray Quality Control (MAQC) project shows inter- and intraplatform reproducibility of gene expression measurements. *Nat Biotechnol* 24(9): 1151-1161, 2006. PMID: 16964229. DOI: 10.1038/nbt1239
  - 21 Hauptman N and Glavač D: Long non-coding RNA in cancer. *Int J Mol Sci* 14(3): 4655-4669, 2013. PMID: 23443164. DOI: 10.3390/ijms14034655
  - 22 Zhou M, Zhao H, Xu W, Bao S, Cheng L and Sun J: Discovery and validation of immune-associated long non-coding RNA biomarkers associated with clinically molecular subtype and prognosis in diffuse large B cell lymphoma. *Mol Cancer* 16(1): 16, 2017. PMID: 28103885. DOI: 10.1186/s12943-017-0580-4
  - 23 Bao S, Zhao H, Yuan J, Fan D, Zhang Z, Su J and Zhou M: Computational identification of mutator-derived lncRNA signatures of genome instability for improving the clinical outcome of cancers: a case study in breast cancer. *Brief Bioinform* 21(5): 1742-1755, 2020. PMID: 31665214. DOI: 10.1093/bib/bbz118
  - 24 Salviano-Silva A, Lobo-Alves SC, Almeida RC, Malheiros D and Petzl-Erler ML: Besides pathology: Long non-coding RNA in cell and tissue homeostasis. *Noncoding RNA* 4(1): 3, 2018. PMID: 29657300. DOI: 10.3390/ncrna4010003
  - 25 Zhou M, Zhao H, Wang Z, Cheng L, Yang L, Shi H, Yang H and Sun J: Identification and validation of potential prognostic lncRNA biomarkers for predicting survival in patients with multiple myeloma. *J Exp Clin Cancer Res* 34: 102, 2015. PMID: 26362431. DOI: 10.1186/s13046-015-0219-5
  - 26 Xiao L, Shi XY, Li ZL, Li M, Zhang MM, Yan SJ and Wei ZL: Downregulation of LINC01508 contributes to cisplatin resistance in ovarian cancer via the regulation of the Hippo-YAP pathway. *J Gynecol Oncol* 32(5): e77, 2021. PMID: 34132072. DOI: 10.3802/jgo.2021.32.e77
  - 27 Trapnell C, Pachter L and Salzberg SL: TopHat: discovering splice junctions with RNA-Seq. *Bioinformatics* 25(9): 1105-1111, 2009. PMID: 19289445. DOI: 10.1093/bioinformatics/btp120
  - 28 Roberts A, Trapnell C, Donaghey J, Rinn JL and Pachter L: Improving RNA-Seq expression estimates by correcting for fragment bias. *Genome Biol* 12(3): R22, 2011. PMID: 21410973. DOI: 10.1186/gb-2011-12-3-r22
  - 29 Son T, Sun J, Choi S, Cho M, Kwon IG, Kim HI, Cheong JH, Choi SH, Noh SH, Woo Y, Fong Y, Park S and Hyung WJ: Multi-institutional validation of the 8th AJCC TNM staging system for gastric cancer: Analysis of survival data from high-volume Eastern centers and the SEER database. *J Surg Oncol* 120(4): 676-684, 2019. PMID: 31338834. DOI: 10.1002/jso.25639
  - 30 Kim E, Ahn B, Oh H, Lee YJ, Lee JH, Lee Y, Kim CH, Chae YS and Kim JY: High Yes-associated protein 1 with concomitant negative LATS1/2 expression is associated with poor prognosis of advanced gastric cancer. *Pathology* 51(3): 261-267, 2019. PMID: 30819540. DOI: 10.1016/j.pathol.2019.01.001
  - 31 Wang L, Feng Z, Wang X, Wang X and Zhang X: DEGseq: an R package for identifying differentially expressed genes from RNA-seq data. *Bioinformatics* 26(1): 136-138, 2010. PMID: 19855105. DOI: 10.1093/bioinformatics/btp612
  - 32 Benjamini Y and Hochberg Y: Controlling the false discovery rate: A practical and powerful approach to multiple testing. *J R Stat Soc Series B Stat Methodol* 57(1): 289-300, 1995. DOI: 10.1111/j.2517-6161.1995.tb02031.x
  - 33 Storey JD and Tibshirani R: Statistical significance for genomewide studies. *Proc Natl Acad Sci U S A* 100(16): 9440-9445, 2003. PMID: 12883005. DOI: 10.1073/pnas.1530509100
  - 34 Djebali S, Davis CA, Merkel A, Dobin A, Lassmann T, Mortazavi A, Tanzer A, Lagarde J, Lin W, Schlesinger F, Xue C, Marinov GK, Khatun J, Williams BA, Zaleski C, Rozowsky J, Röder M, Kokocinski F, Abdelhamid RF, Alioto T, Antoshechkin I, Baer MT, Bar NS, Batut P, Bell K, Bell I, Chakraborty Y, Chen X, Chrast J, Curado J, Derrien T, Drenkow J, Dumais E, Dumais J, Duttagupta R, Falconnet E, Fastuca M, Fejes-Toth K, Ferreira P, Foissac S, Fullwood MJ, Gao H, Gonzalez D, Gordon A, Gunawardena H, Howald C, Jha S, Johnson R, Kapranov P, King B, Kingswood C, Luo OJ, Park E, Persaud K, Preall JB, Ribeca P, Risk B, Robyr D, Sammeth M, Schaffer L, See LH, Shahab A, Skancke J, Suzuki AM, Takahashi H, Tilgner H, Trout D, Walters N, Wang H, Wrobel J, Yu Y, Ruan X, Hayashizaki Y, Harrow J, Gerstein M, Hubbard T, Reymond A, Antonarakis SE, Hannon G, Giddings MC, Ruan Y, Wold B, Carninci P, Guigó R and Gingeras TR: Landscape of transcription in human cells. *Nature* 489(7414): 101-108, 2012. PMID: 22955620. DOI: 10.1038/nature11233
  - 35 Ba MC, Long H, Cui SZ, Gong YF, Yan ZF, Wu YB and Tu YN: Long noncoding RNA LINC00673 epigenetically suppresses KLF4 by interacting with EZH2 and DNMT1 in gastric cancer. *Oncotarget* 8(56): 95542-95553, 2017. PMID: 29221147. DOI: 10.18632/oncotarget.20980



- 36 Matouk IJ, DeGroot N, Mezan S, Ayesh S, Abu-lail R, Hochberg A and Galun E: The H19 non-coding RNA is essential for human tumor growth. *PLoS One* 2(9): e845, 2007. PMID: 17786216. DOI: 10.1371/journal.pone.0000845
- 37 Gutschner T, Hämmerle M, Eissmann M, Hsu J, Kim Y, Hung G, Revenko A, Arun G, Stentrup M, Gross M, Zörnig M, MacLeod AR, Spector DL and Diederichs S: The noncoding RNA MALAT1 is a critical regulator of the metastasis phenotype of lung cancer cells. *Cancer Res* 73(3): 1180-1189, 2013. PMID: 23243023. DOI: 10.1158/0008-5472.CAN-12-2850
- 38 Liu K, Gao L, Ma X, Huang JJ, Chen J, Zeng L, Ashby CR Jr, Zou C and Chen ZS: Long non-coding RNAs regulate drug resistance in cancer. *Mol Cancer* 19(1): 54, 2020. PMID: 32164712. DOI: 10.1186/s12943-020-01162-0
- 39 Gao S, Zhao ZY, Wu R, Zhang Y and Zhang ZY: Prognostic value of long noncoding RNAs in gastric cancer: a meta-analysis. *Onco Targets Ther* 11: 4877-4891, 2018. PMID: 30147339. DOI: 10.2147/OTT.S169823
- 40 Ye H, Liu K and Qian K: Overexpression of long noncoding RNA HOTTIP promotes tumor invasion and predicts poor prognosis in gastric cancer. *Onco Targets Ther* 9: 2081-2088, 2016. PMID: 27103834. DOI: 10.2147/OTT.S95414
- 41 Li J, Gao J, Tian W, Li Y and Zhang J: Long non-coding RNA MALAT1 drives gastric cancer progression by regulating HMGB2 modulating the miR-1297. *Cancer Cell Int* 17: 44, 2017. PMID: 28396617. DOI: 10.1186/s12935-017-0408-8
- 42 Karagkouni D, Paraskevopoulou MD, Tastsoglou S, Skoufos G, Karavangeli A, Pierros V, Zacharopoulou E and Hatzigeorgiou AG: DIANA-LncBase v3: indexing experimentally supported miRNA targets on non-coding transcripts. *Nucleic Acids Res* 48(D1): D101-D110, 2020. PMID: 31732741. DOI: 10.1093/nar/gkz1036
- 43 Rao AKDM, Rajkumar T and Mani S: Perspectives of long non-coding RNAs in cancer. *Mol Biol Rep* 44(2): 203-218, 2017. PMID: 28391434. DOI: 10.1007/s11033-017-4103-6
- 44 Camacho CV, Choudhari R and Gadad SS: Long noncoding RNAs and cancer, an overview. *Steroids* 133: 93-95, 2018. PMID: 29317255. DOI: 10.1016/j.steroids.2017.12.012
- 45 Hermeking H: MicroRNAs in the p53 network: micromanagement of tumour suppression. *Nat Rev Cancer* 12(9): 613-626, 2012. PMID: 22898542. DOI: 10.1038/nrc3318
- 46 Nie D, Fu J, Chen H, Cheng J and Fu J: Roles of microRNA-34a in epithelial to mesenchymal transition, competing endogenous RNA sponging and its therapeutic potential. *Int J Mol Sci* 20(4): 861, 2019. PMID: 30781524. DOI: 10.3390/ijms20040861
- 47 Hui WT, Ma XB, Zan Y, Wang XJ and Dong L: Prognostic significance of MiR-34a expression in patients with gastric cancer after radical gastrectomy. *Chin Med J (Engl)* 128(19): 2632-2637, 2015. PMID: 26415802. DOI: 10.4103/0366-6999.166019
- 48 Wang P, Zhai G and Bai Y: Values of miR-34a and miR-218 expression in the diagnosis of cervical cancer and the prediction of prognosis. *Oncol Lett* 15(3): 3580-3585, 2018. PMID: 29456728. DOI: 10.3892/ol.2018.7791
- 49 Ren F, Zhang X, Liang H, Luo D, Rong M, Dang Y and Chen G: Prognostic significance of MiR-34a in solid tumors: a systemic review and meta-analysis with 4030 patients. *Int J Clin Exp Med* 8(10): 17377-17391, 2015. PMID: 26770329.
- 50 Huang Y, Zou Y, Lin L, Ma X and Chen H: Identification of serum miR-34a as a potential biomarker in acute myeloid leukemia. *Cancer Biomark* 22(4): 799-805, 2018. PMID: 29945348. DOI: 10.3233/CBM-181381
- 51 Orangi E and Motovali-Bashi M: Evaluation of miRNA-9 and miRNA-34a as potential biomarkers for diagnosis of breast cancer in Iranian women. *Gene* 687: 272-279, 2019. PMID: 30468908. DOI: 10.1016/j.gene.2018.11.036
- 52 Imani S, Zhang X, Hosseini-fard H, Fu S and Fu J: The diagnostic role of microRNA-34a in breast cancer: a systematic review and meta-analysis. *Oncotarget* 8(14): 23177-23187, 2017. PMID: 28423566. DOI: 10.18632/oncotarget.15520
- 53 Lang B, Armaos A and Tartaglia GG: RNAct: Protein-RNA interaction predictions for model organisms with supporting experimental data. *Nucleic Acids Res* 47(D1): D601-D606, 2019. PMID: 30445601. DOI: 10.1093/nar/gky967
- 54 Ochi Y, Chano T, Ikebuchi K, Inoue H, Isono T, Arai A, Tameno H, Shimada T, Hisa Y and Okabe H: RB1CC1 activates the p16 promoter through the interaction with hSNF5. *Oncol Rep* 26(4): 805-812, 2011. PMID: 21637919. DOI: 10.3892/or.2011.1329
- 55 Ikebuchi K, Chano T, Ochi Y, Tameno H, Shimada T, Hisa Y and Okabe H: RB1CC1 activates the promoter and expression of RB1 in human cancer. *Int J Cancer* 125(4): 861-867, 2009. PMID: 19437535. DOI: 10.1002/ijc.24466
- 56 Demidenko R, Razanauskas D, Daniunaite K, Lazutka JR, Jankevicius F and Jarmalaite S: Frequent down-regulation of ABC transporter genes in prostate cancer. *BMC Cancer* 15: 683, 2015. PMID: 26459268. DOI: 10.1186/s12885-015-1689-8
- 57 Elsnerova K, Bartakova A, Tihlarik J, Bouda J, Rob L, Skapa P, Hrudá M, Gut I, Mohelnikova-Duchonova B, Soucek P and Václavikova R: Gene expression profiling reveals novel candidate markers of ovarian carcinoma intraperitoneal metastasis. *J Cancer* 8(17): 3598-3606, 2017. PMID: 29151946. DOI: 10.7150/jca.20766
- 58 Gillet JP, Schneider J, Bertholet V, DE Longueville F, Remacle J and Efferth T: Microarray expression profiling of ABC transporters in human breast cancer. *Cancer Genomics Proteomics* 3(2): 97-106, 2006. PMID: 31394687.
- 59 Deng J, Zhang T, Liu F, Han Q, Li Q, Guo X, Ma Y, Li L and Shao G: CRL4-DCAF8L2 E3 ligase promotes ubiquitination and degradation of BARD1. *Biochem Biophys Res Commun* 611: 107-113, 2022. PMID: 35487060. DOI: 10.1016/j.bbrc.2022.04.100
- 60 Wang H, Luo J, Tian X, Xu L, Zhai Z, Cheng M, Chen L and Luo S: DNAJC5 promotes hepatocellular carcinoma cells proliferation through regulating SKP2 mediated p27 degradation. *Biochim Biophys Acta Mol Cell Res* 1868(6): 118994, 2021. PMID: 33662413. DOI: 10.1016/j.bbamcr.2021.118994
- 61 Arayataweegool A, Srisuttee R, Bin-Alee F, Mahattanasakul P, Tangjaturonrasme N, Kerekhanjanarong V, Mutirangura A and Kitkumthorn N: Induction of ZCCHC6 expression in peripheral blood mononuclear cells by HNSCC secretions. *Gene* 754: 144880, 2020. PMID: 32526260. DOI: 10.1016/j.gene.2020.144880
- 62 El Hadidy N and Uversky VN: Intrinsic disorder of the BAF complex: Roles in chromatin remodeling and disease development. *Int J Mol Sci* 20(21): 5260, 2019. PMID: 31652801. DOI: 10.3390/ijms20215260

Received August 8, 2022

Revised September 21, 2022

Accepted September 26, 2022